MPSBL:Multiple Transmit Power Assisted Sequence-based Localization in Wireless Sensor Networks

Fujuan Guo Mehmet C. Vuran
Computer Science and Engineering
University of Nebraska-Lincoln
Lincoln, USA
{fguo,mcvuran}@cse.unl.edu

Kanghyeok Yang
Construction Engineering and Management
University of Nebraska-Lincoln
Lincoln, USA
kyang12@huskers.unl.edu

Changbum R. Ahn
Construction Science
Texas A & U University
College Station, USA
ryanahn@arch.tamu.edu

***Abstract*—Construction workers who usually work in high altitudes and hazardous construction zones are prone to accidents that may lead to injuries and fatalities. This calls for advanced monitoring technologies that can locate workers *and* hazardous areas within a dynamically evolving outdoor/indoor area. More accurate localization techniques indicate more safety for protecting them from an accident. In this paper, a multiple transmit power assisted sequence-based localization (MPSBL) solution is developed to achieve high localization accuracy. The theoretical analysis and system model design illustrate the feasibility of MPSBL. Simulations and empirical experiments in construction zones have been conducted, which show that MPSBL outperforms state-of-the-art approaches.**

I. Introduction

The construction industry is considered as one of the most dangerous industries in the United States [1]. Ironworkers who are working on narrow surfaces of structural steel beams at the great height face the highest lifetime risk of fatal injuries. To protect the safety of workers among all the construction trades, it is necessary to take action in many aspects, such as, add guardrails, safety nets, and personal protective equipment. In [2], we have designed a semi-supervised near-miss fall detection solution for a wearable system, which can automatically detect near-miss falls based on worker kinematic data. Based on this near-miss data, reasons for potential accidents can be identified. Furthermore, we have proposed a collective sensing approach that senses workers' gait abnormality patterns to identify the physical hazards [3]. This approach is refined by adding two-dimensional spatial information for the application toward general construction trades [4]. As a part of those works, in this paper, we focus on designing a more accurate localization system for hazard location identification such that workers and management can be alerted.

The developed approach belongs to a class of sequence-based localization (SBL) approaches [5], which provides three main advantages: (1) SBL can provide a relatively higher localization accuracy compared to range-based approaches; (2) SBL has the ability to mitigate channel fading and shadowing problems; and (3) compared to fingerprinting approaches, SBL is a pre-data free approach which saves a lot of time for collecting training data [6]. These features are attractive for localization applications in construction zones where fingerprinting may not be possible and the environment (hence, fading and shadowing sources) may change dynamically with construction phases.

Although SBL reduces channel effects to a large degree, the accuracy of SBL is still affected by rank match error problem due to channel noise and multiple match situation when multiple maximum coefficient values exist (Multiple-maximum-τ problem) [5], [7], [8]. To tackle this problem, in this paper, we design a novel multiple transmit power assisted SBL (MPSBL) approach in wireless sensor networks for construction zone localization, which is an improvement of SBL algorithm. The key idea behind MPSBL approach is that instead of using equal received signal strength (RSS) locus generated by equal transmit power of a pair of nodes, MPSBL utilizes multiple transmit power levels to generate equal RSS locus to partition the localization area. Since the equal RSS locus is a circle under the circumstance of non-equal transmit power [9], compared to the traditional SBL, the localization granularity for the same localization area could be smaller. More importantly, transmit power diversity allows more RSSI value constraints to be involved, determining the most likely estimation values, which increases localization accuracy and precision. The main contributions of this paper are summarized as below:

- We propose a multiple transmit power assisted SBL approach, which is novel and can significantly improve the performance of traditional SBL approaches.
- We have designed the system model of MPSBL approach.
- To address SBL's multiple-maximum-τ problem, we provide two types of approaches: MPSBL Most Frequency First (MPSBL-MFF) and MPSBL Filtered Weighted Average (MPSBL-FWA). By applying them, the detrimental impact of multiple-maximum-τ problem has been mitigated.
- Various of simulations and a real-world experiment in a construction zone have been conducted to evaluate MPSBL and compare its two flavors. The results convey that MPSBL outperforms the state-of-the-art significantly at both theoretical and practical aspects.

The rest of the paper is organized as follows: Section II reviews the related work. Section III presents the design of the MPSBL system mode and two MPSBL flavors, MPSBL-MFF and MPSBL-FWA. Simulation and experiment results

978-1-5386-3180-5/18/$31.00 ©2018 IEEE

are described in Section IV and Section V, respectively. We conclude the paper in Section VI.

II. Related work

In recent years, numerous localization algorithms have been developed to enhance indoor localization performance [10]–[12]. Fingerprinting is one of the popular approaches that is not only limited to received signal strength information but also includes other sources of information to create a fingerprint map [13]. For example in [13], a novel approach that combines an extended Kalman filter and a fingerprinting navigation algorithm is developed. Instead of only using RSSI information for fingerprinting, the inertial measurement unit (IMU) information is involved to estimate location and perform navigation in real-time in an indoor environment. In [14], the mean RSS value collected from different frequencies is utilized as fingerprint information. By using this information, the position error is improved 70% compared with only using an inertial navigation system (INS). In addition to RSS, operation frequency, transmit power, channel state information (CSI), and other physical layer parameters have been utilized for high-accuracy localization. In [15], it is proven that all RSS-based localization algorithms can be improved by leveraging RSS information obtained from multiple frequencies and powers. CSI-MIMO, as a fingerprint signature, has been used for indoor localization in [16]. The frequency and spatial diversity result in a 50% accuracy of localization than the simple fine-grained indoor fingerprint system. Although utilizing multiple frequencies, transmit power, and CSI achieves higher localization accuracy, these solutions are still based on fingerprinting approaches. However, fingerprint techniques are computationally complex and costly due to calculation and pre-collecting data required. More importantly, in a dynamically evolving environment such as construction zones, fingerprinting is cost prohibitive due to the frequent need for fingerprinting when environment parameters change.

Compared to fingerprinting approaches, SBL is a low computation-complexity and a highly efficient approach. In [5], SBL is first developed as *Ecolocation* and in [7], this approach is refined. The results show that SBL outperforms RSS-based localization approaches. The key parameter that impacts SBL is *Kendall's correlation coefficient* (τ) and several improvements to the original SBL is developed to improve utilization of τ. For example in [8], a weighted rank order correlation coefficient and a dynamic centroid method are used. However, these approaches are still limited to a single transmit power level and is based on averaging selected three candidates, which leads to a slight improvement. In this paper, we focus on operating both on the τ metric and the coordinates of centroid points with multiple transmit powers, which enhances the localization accuracy dramatically.

Recently, the traditional SBL algorithm has been improved by changing the transmit power from uniform to non-uniform transmit power levels (NU-SBL) [9], which potentially has a higher localization accuracy than the traditional SBL approach [5], [7]. However, this work only focuses on the simulation for exploring optimizing the deployment of beacons, and experimental verifications are not provided. More importantly, to the best of our knowledge a specific algorithm that utilizes multiple transmit power levels has not been designed for SBL-class localization algorithms. In this paper, we propose a multiple transmit power assisted SBL algorithm, design the system model and analyze the feasibility and localization accuracy through both simulations and real-world experiments. As we discuss below, the accuracy of localization is improved significantly compared to the state of the art.

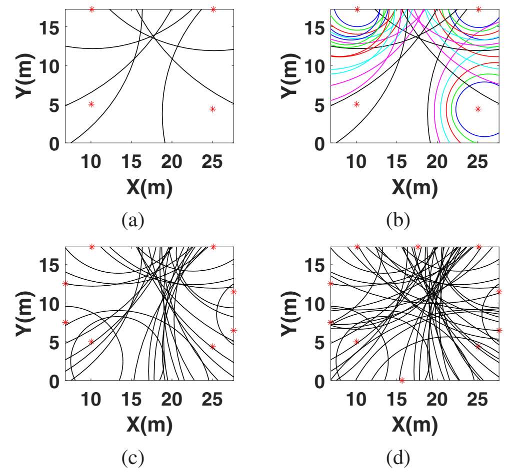

Fig. 1. (a) Four beacons with a single $\Delta\rho$, (b) Four beacons with multiple $\Delta\rho$s, (c) Eight beacons with a single $\Delta\rho$ (d) Ten beacons with a single $\Delta\rho$.

III. Multiple Transmit Power Assisted Sequence Based Localization (MPSBL)

A. MPSBL Features

For the following discussion, we assume the reader is familiar with the SBL and NU-SBL approaches [5], [7], [9]. The main features of the MPSBL approach can be illustrated in Figs. 1, where red star markers represent beacons. When RSS from two beacons, with unequal transmit powers, are compared, the equal-RSS locus, which is the set of points where RSS from both beacons are equal, divides the area into two faces. For unequal transmit power, the equal-RSS locus is a circle. The lines in Figs. 1 with different colors denote equal-RSS locus generated by different transmit power difference values. We denote the transmit power difference by $\Delta\rho$. (1) When unequal transmit power levels are used, equal-RSS locus is a circle instead of a straight line, which can potentially increase the localization accuracy because of the smaller granularity caused by an increase in the number of faces (Fig. 1(a)) [9]; (2) The granularity can be controlled not only by increasing the number of beacons (Fig. 1(c)-1(d)) but also by using multiple transmit power differences ($\Delta\rho$) (Fig. 1(b)); (3) The localization accuracy can be improved by **transmit power difference diversity**. More specifically, the number of faces depends on the number of unique transmit power differences, but not on the specific values of transmit powers. Therefore, multiple transmit power levels with the same difference, $\Delta\rho$, can be used to alleviate random effects of the channel, and improve accuracy with higher probability. (4) Compared to SBL, MPSBL uses RSS and radius constraints instead of rank order of beacons to determine an estimated face. Thus, the localized position is not relevant to the physical distance to the beacon node. Instead, it depends on the $\Delta\rho$ and radius of the circles surrounding each region.

B. Terminology

We assume that a set $\mathcal{Q} = \{q : q \in [1, Q]\}$ of Q beacon nodes, and correspondingly N pairs of beacons, where $N = \binom{Q}{2}$, exist. Each beacon node periodically transmits P beacons with transmit powers from a set $\mathcal{P} = \{\rho_1, \ldots, \rho_p, \ldots, \rho_P\}$. Consequently, a node receives up to $Q \times P$ beacons for localization in each turn.

From the transmit power set, $\mathcal{P}$, a sequence of transmit power differences can be generated as $\Delta\mathcal{P}' = \{\Delta\rho'_1, \ldots, \Delta\rho'_m, \ldots, \Delta\rho'_M\}$, where $M = P(P-1)/2$. Note that the elements of the transmit power set generally depends on the transmit power levels specified in the radio module of the beacon node. Consequently, the differences between each transmit power level cannot be controlled arbitrarily. As a result, several elements of $\Delta\mathcal{P}'$ can be equal to each other. From $\Delta\mathcal{P}'$, we define two sets: $\Delta\mathcal{P} = \{\rho_k \in \Delta\mathcal{P}' : \rho_k$ is distinct $\}$ includes the distinct transmit power differences, and $\Theta = \{\theta_1, \ldots, \theta_k, \ldots, \theta_K\}$ includes the number of occurances of each distinct transmit power difference, ρ_k, in $\Delta\mathcal{P}'$ and $|\Delta\mathcal{P}| = |\Theta| = K \leq M$. This results in a transmit power difference diversity of $M - K$.

For example, for a transmit power set of $\{1, 3, 4, 5\}$; $\Delta\mathcal{P}' = \{2, 3, 4, 1, 2, 1\}$, $\Delta\mathcal{P} = \{1, 2, 3, 4\}$, and $\Theta = \{2, 2, 1, 1\}$, with a diversity of 2.

Each beacon pair, from a pair of beacon nodes, n, with a distinct transmit power difference, ρ_k, results in a distinct equal-RSS locus, which is a circle if the transmit power difference is nonzero. Accordingly, $K \times N$ such loci can be generated with the above formulation. We denote the area within such circles as $\mathbb{A}_{k,n}$. Intersections of these loci partition the area into C faces and each face is represented by its centroid point, which results in a set of centroid points, $\mathcal{C}$, with coordinates, $(x_c, y_c), \forall c \in \mathcal{C}$[1].

As detailed below, the goal of the localization algorithm is to find a probability measure of the proximity of the node to each centroid point, and accordingly, estimate the node location.

C. MPSBL Algorithm

MPSBL consists of three phases: (1) The *pre-localization phase* is used to establish constraint sequences associated with a centroid point of each partitioned face. In this phase, a constraint table, $\mathbb{E}$, is generated for the location site. Compared to fingerprinting, this phase requires only path loss statistics, and can be conducted offline once, or only when environment parameters change significantly (e.g., during different stages of construction). (2) In the *measurement phase*, RSS information from received beacons with different transmit powers is used to establish a node constraint matrix. (3) In *location estimation phase*, each constraint sequence (row vector of the constraint matrix in Phase 2) is compared to the constraint table to establish a probability matrix of the node location with respect to centroid points. Accordingly, the node location is estimated through two distinct approaches. The details of each phase are discussed next.

1) Pre-localization Phase: In this phase, a constraint table $\mathbb{E} = \{\mathbf{L}_1, \ldots, \mathbf{L}_c, \ldots, \mathbf{L}_C\}$, as a set of constraint matrices $\mathbf{L}_c$ for each face c, is constructed. For a given centroid point, c, the constraint matrix is an $N \times K$ matrix, given by:

$$\mathbf{L}_c = (l_{c,n,k}), \text{ where } l_{c,n,k} \triangleq \begin{cases} 1, & c \in \mathbb{A}_{k,n} \\ -1, & c \notin \mathbb{A}_{k,n}. \end{cases} \quad (1)$$

For a given face, c, each column vector, $\mathbf{l}_{c,k}$, in $\mathbf{L}_c$ specifies a set of constraints for the centroid point of the face with respect to a transmit power difference, ρ_k.

2) Measurement Phase: In the measurement phase, based on its RSS measurements from Q beacon nodes with P transmit power levels, the node constructs a measurement matrix, $\mathbf{\Gamma}$ as:

$$\mathbf{\Gamma} = \begin{bmatrix} \gamma_{1,1} & \cdots & \gamma_{1,Q} \\ \vdots & \ddots & \vdots \\ \gamma_{P,1} & \cdots & \gamma_{P,Q} \end{bmatrix}, \quad (2)$$

where each row vector, $\boldsymbol{\gamma}_p^T$, represents the RSS values received from all beacons with a transmit power level ρ_p.

Now, for each transmit power difference, $\Delta\rho_k$, the node compares the RSS readings between each pair of beacon nodes, to create a $\theta_k \times N$ node constraint matrix:

$$\mathbf{\Lambda}_k = (\lambda_{k,r,n}), \quad (3)$$

where $r \in [1, \theta_k]$ and $n \in [1, N]$. Let beacon pair n consists of beacon nodes n_1 and n_2 and row r corresponds to $\Delta\rho_k = \rho_{r_1} - \rho_{r_2}$. Then,

$$\lambda_{k,r,n} \triangleq \begin{cases} 1, & \gamma_{r_1,n_1} \geq \gamma_{r_2,n_2} \\ -1, & \gamma_{r_1,n_1} < \gamma_{r_2,n_2}. \end{cases} \quad (4)$$

For a given transmit power difference, $\Delta\rho_k$, each row vector, $\boldsymbol{\lambda}_{k,r}^T$ of $\mathbf{\Lambda}_k$ constitutes an independent constraint sequence for the location estimation. Since there are multiple pairs of transmit power level that correspond to a $\Delta\rho_k$ (θ_k of them), the localization accuracy can be improved. This is the main advantage of the MPSBL approach. Additionally, the size θ_k depends on $\Delta\rho_k$ and the construction of the transmit power set $\mathcal{P}$. Therefore, there are K constraint matrices with the same column size but different row sizes. The entire set of node constraints can then be written as $\mathbf{\Lambda} = \{\mathbf{\Lambda}_1, \ldots, \mathbf{\Lambda}_k, \ldots, \mathbf{\Lambda}_K\}$.

3) Location Determination Phase: In this phase, the node constraints, $\mathbf{\Lambda}$, in Phase 2 are compared to the constraint set, $\mathbb{E}$, in Phase 1, to find a probability of the proximity of the node to each centroid point. We adopt *Kendall's Tau* as the metric for this comparison [17]. Basically, this comparison results in the correlation between two sequences. The range

[1]We use c to denote a face and its corresponding centroid point interchangeably.

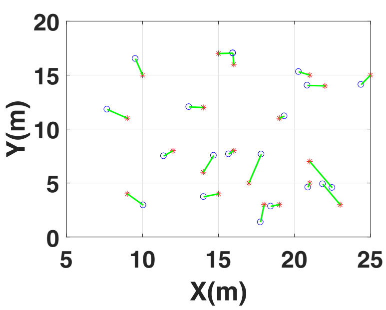

(a)

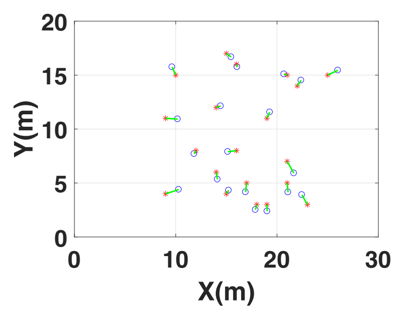

(b)

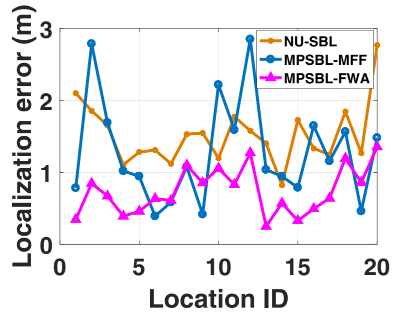

(c)

Fig. 2. Estimation and ground truth for (a) MPSBL-MFF and (b) MPSBL-FWA, (c) Localization error of NU-SBL, MPSBL-MFF, and MPSBL-FWA.

of the τ value is $[-1, 1]$, where a higher τ value indicates a better match.

For a given transmit power difference, $\Delta\rho_k$, we find the correlation between each constraint sequence, $\boldsymbol{\lambda}_{k,r}^T$, in (3) and $\mathbf{l}_{c,k}$ $\forall c \in [1, C]$ in (1) using (13) in [7]. The results are used to construct the following $\theta_k \times C$ matrix:

$$\boldsymbol{T}_k = \begin{bmatrix} \tau_{1,1} & \cdots & \tau_{1,c} & \cdots & \tau_{1,C} \\ \vdots & \ddots & \vdots & \ddots & \vdots \\ \tau_{\theta_k,1} & \cdots & \tau_{\theta_k,c} & \cdots & \tau_{\theta_k,C} \end{bmatrix} \tag{5}$$

Each row of $\boldsymbol{T}_k$ gives a measure of how close the node is to each of the centroid points for the pair of transmit power levels that have a difference of $\Delta\rho_k$. In theory, the maximum τ value of each row would indicate the best centroid point for estimation. Moreover, in theory, the best centroid point for each row would be the *same* point.

In practice, randomness in the channel due to shadowing and fading results in two issues: First, in a given row of $\boldsymbol{T}_k$, there may be multiple maximum τ values. Furthermore, the set of centroid points with the maximum τ value(s) may be different for each row. We address these issues with two approaches as discussed next.

D. Most Frequent First

The maximum τ value from each row in (5) indicates centroid point(s) that are highly likely to be in the node's proximity. For each row, those centroid points with the maximum τ value are placed in a candidate vector $\boldsymbol{c}_m$. In SBL [5], a simple average of the coordinates of all candidate centroid points is used as the estimation. However, this approach may increase estimation error since outliers are included in the average. Instead, we exploit the diversity provided by transmit power differences to improve the estimation accuracy. In the most frequent first (MFF) approach, the centroid point, which has been selected as a candidate by each row with the most frequency, is selected as the location estimation. The centroid point with the highest values τs is selected if there are multiple such centroid points. We refer to this algorithm as *MPSBL-MFF*.

E. Filtered Weighted Average

MPSBL-MFF eventually selects a single centroid point coordinate as the location estimation. Hence, the location error depends on the resolution created by the number of centroid points. Moreover, information from other centroid points with high τ values is eliminated in MPSBL-MFF since only the *maximum* τ values contribute to the most frequency centroid point are considered. To address this issue, we follow a filtered weighted average approach. In this case, for each $\Delta\rho_k$, all the maximum τ values from each row of $\boldsymbol{T}_k$ are placed in a candidate vector $\boldsymbol{\tau}_m$, which is first filtered to a vector $\boldsymbol{\tau}_{k,th}$ such that only τ values above a certain threshold τ_{th} are kept. When combined for all $\Delta\rho_k$ values, this results in a corresponding vector of centroid points, $\boldsymbol{c}_{th} \subset \mathcal{C}$ with a sufficiently high correlation with the node's location. We then use the τ value of each centroid point as a weight to its location and find the location estimation as a weighted average of all such centroid points. Accordingly, the location estimation, $(\hat{x}, \hat{y})$, is expressed by:

$$(\hat{x}, \hat{y}) = \sum_{c \in \boldsymbol{c}_{th}} \frac{\tau_c(x_c, y_c)}{\sum_{i \in \boldsymbol{c}_{th}} \tau_c} \tag{6}$$

where τ_c represents the τ value in set $\boldsymbol{\tau}_{k,th}$ corresponding to centroid point c. Note that the same centroid point can be included in the weighted average multiple times if sufficiently high τ values are calculated for that point in multiple rows of $\boldsymbol{T}_k$ $\forall k$. This would shift the estimation location towards that centroid point. We refer to this algorithm as *MPSBL-FWA*.

IV. Simulation Results

A. Simulation Methodology

We conduct simulations to evaluate the effectiveness and validity of MPSBL. The widely used log-normal shadowing model is adopted to generate RSS samples. The parameters closely follow [5], except the transmit power. We utilize 10 transmit power levels from $10dBm$ to $-17dBm$, and we assume 30 beacon nodes are in the radio range of each other for all transmit power levels.

Two types of simulation evaluations are performed. First, we simulate a random network of 20 nodes to localize and compare the performance of MPSBL (MPSBL-MFF and MPSBL-FWA) with state-of-the-art approaches. Finally, the key parameters related to the performance of MPSBL, including path loss exponent and transmit power difference, are investigated. In this paper, we use the localization error and localization precision defined in [5] to evaluate the performance of each approach.

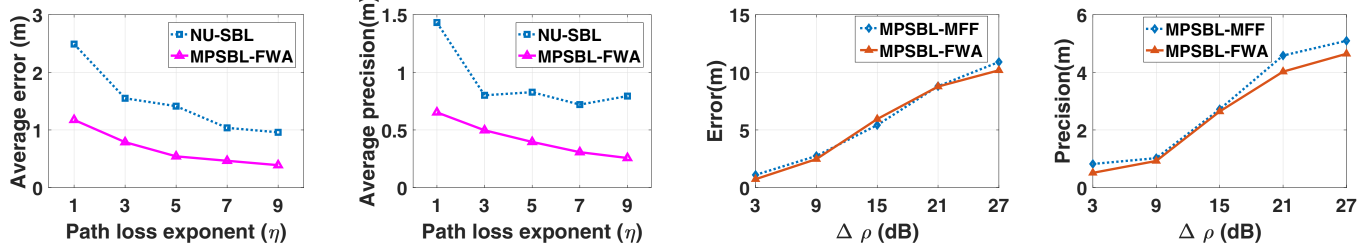

(a) (b) (c) (d)

Fig. 4. (a) Average error and (b) average precision w.r.t. path loss exponent. (c) Average error and (d) precision w.r.t. transmit power difference, $\Delta\rho$.

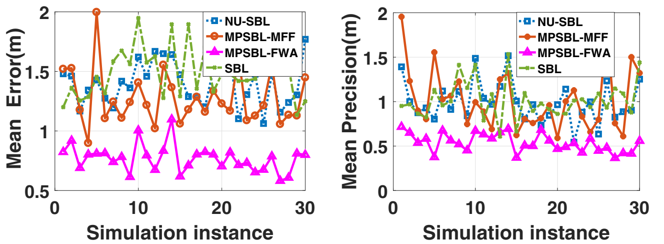

(a) (b)

Fig. 3. (a) The mean error and (b) mean precision of NU-SBL, SBL, MPSBL-MFF, and MPSBL-FWA.

B. MPSBL Performance and Comparison

We compare MPSBL with two state-of-the-art approaches: SBL [7] and NU-SBL [9]. To this end, we randomly generate 20 points to be located in an area and operate MPSBL-MFF, MPSBL-FWA, and NU-SBL algorithms. The results are presented in Figs. 2. In Figs. 2(a)-2(b) the estimated and actual locations of a random set of 20 points are shown for MPSBL-MFF and MPSBL-FWA, respectively. It can be observed that, most of the estimation points by MPSBL-FWA in Fig. 2(b) are closer to their ground truth than those in Fig. 2(a). This indicates that the MPSBL-FWA has a better performance than MPSBL-MFF. In Fig. 2(c), localization error for each 20 point of NU-SBL is shown along with these two approaches. It can be observed that MPSBL-FWA performs best among these three and most estimations of MPSBL-MFF have a lower localization error than NU-SBL.

In Figs. 2, the performance of MPSBL for a single realization is shown to illustrate the variance among localized points, where MPSBL-FWA has a lower variance. Next, we present the results of a simulation study with 30 realizations of the 20-node random topology for MPSBL-MFF, MPSBL-FWA, NU-SBL and SBL. The simulation results in terms of the mean localization error and mean precision related for each simulation instance is presented in Figs. 3(a)-3(b), respectively. Based on the result shown in Figs. 3, it can be observed that MPSBL-FWA has both the lowest mean error and precision compared to other three protocols. Except for two instances, the average localization error is sub-meter. Moreover, MPSBL-FWA precision outperforms the other three in 27 times out of 30 instances, excluding three tie points. Although the MPSBL-MFF performs worse than MPSBL-FWA, it is still better than the SBL and NU-SBL approach in terms of most of the points better than NU-SBL and SBL approach on both localization error and precision. Considering its relatively low computation complexity in estimation, MPSBL-MFF can be used in resource-constrained nodes with acceptable performance.

Based on the above analysis, we can conclude that both MPSBL-MFF and MPSBL-FWA can leverage the transmit power different diversity and obtain a better performance than NU-SBL and SBL. Statistically, the MPSBL-MFF improves the localization accuracy by 9.26% compared to NU-SBL. On the other hand, MPSBL-FWA improves localization accuracy by up to 45.28% compared to NU-SBL, and 48.1% compared to SBL, in terms of mean localization error.

C. Parameter Analysis

1) Path loss: Path loss is an essential parameter for localization in evolving construction zones. We investigate how the path loss effects MPSBL by simulations and compare to NU-SBL. Specifically, the localization error and precision vary with the path loss exponent are illustrated in Fig. 4(a) and Fig. 4(b). As can be seen in these two figures, both the localization error and precision of MPSBL-FWA and NU-SBL have decreasing trends with increasing path loss exponent. This can mainly be attributed to diminishing multi-path effects with increasing path loss exponent. MPSBL-FWA performs better than NU-SBL for all path loss exponent range from 1 to 9, which highlights the advantages of the MPSBL approach.

2) Transmit Power Difference: We conduct a simulation by varying the $\Delta\rho$ to evaluate the relationship between the $\Delta\rho$ and localization performance. Based on our simulation environment, there are ten transmit power levels ranging from 10dBm to -17dBm with a gap of 3dB. The $\Delta\rho$ values from 3dB to 27dB related to the mean localization error and precision are in Fig. 4(c) and Fig. 4(d), respectively. As can be seen, both the localization error and precision have an increasing trend with $\Delta\rho$ values. This is also one of the reasons for selecting 3dBm $\Delta\rho$ to operate simulations in this paper.

Intuitively, the $\Delta\rho$ also affects area partitioning. Since the larger $\Delta\rho$ indicates the smaller radius of equal RSS locus, for a specific area, adjusting the $\Delta\rho$ can benefit the desired region. This provides an idea of designing a dynamic localization approach based on MPSBL, which is left for a future work.

V. Experiment Results

A. Experiment setup

We conduct an experiment in an indoor construction zone with a size of 27.62×17.25 m^2 filled with furniture, walls, and construction equipment. The experiment environment is shown in Fig. 5. Wizzimote, a MSP430 microcontroller-based

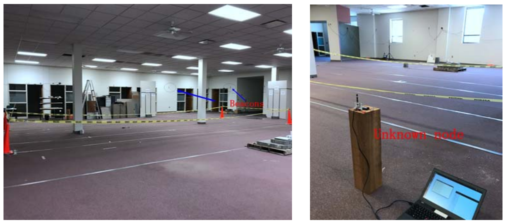

(a) (b)

Fig. 5. (a) The experiment site with deployed beacons surrounded (b) Unknown node collecting data from beacons

SoC with a CC1101 RF transceiver, is used to carry out this experiment and all the collected data is synchronized [18]. The collected data is time-stamped through the time on the laptop based on the network time protocol. 30 beacon nodes along the four walls of the room, at a height of $2.2m$, are deployed. The unknown node is a receiver which collects the information including beacon node ID, RSS value, and transmit power level corresponding to the received message. Based on the above setting, a static experiment is conducted in six locations.

B. Results

1) Path Loss Exponent Estimation: We first estimate the path loss exponent based on the experiment data before performing localization, using a Minimum Mean Square Error estimator [19]. The estimated result is 3.36. Alternatively, we also employ the simulation model to generate the ideal RSS value to fit with the experimental data, which results in a close value with the previous estimation. Therefore, we consider 3.4 as the path loss exponent for our experiment scenario.

2) Localization Results: We run MPSBL-FWA, MPSBL-MFF, and NU-SBL simultaneously based on the experimental data. The results of the empirical mean localization error are shown in Fig. 6. It can be observed that MPSBL-FWA has a $0.434m$ lower error than NU-SBL and MPSBL-MFF performs $0.267m$ better than NU-SBL, which suggests that MPSBL approach is also efficient in practice to solve the multiple-maximum-τ problem and achieve higher localization accuracy.

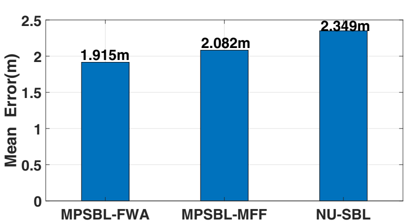

Fig. 6. Localization error due to NU-SBL, MPSBL-MFF and MPSBL-FWA for the indoor experiment

In practice, the construction zone is a complex environment, which can be imitated as an indoor and outdoor mixed environment. Investigation of multiple types of indoor/outdoor construction scenarios is left for future work.

VI. Conclusion

MPSBL leverages multiple transmit power difference diversity to enhance SBL approach for localization in WSNs. In this paper, the system model with two flavors of algorithms has been developed. Various of simulations and an indoor experiment have been conducted. Both results show that the MPSBL outperforms the state-of-the-art approaches. Moreover, MPSBL can focus on an interested area by operating transmit power differences without any topology change. This provides a potential methodology for the dynamic localization implementation in a construction zone. We consider this as a future work. Therefore, we believe that the MPSBL is a very promising and efficient methodology for localization.

VII. Acknowledgments

This work is supported in part by US National Science Foundation grants NSF CIS-1538029 and NSF CNS-1423379, and the R&D Program funded by the Ministry of Land, Infrastructure, and Transport of the Korean government [17CTAP-C128499-01].

References

[1] BLS, "Bureau of labor statistics," 2013.

[2] K. Yang, C. R. Ahn, M. C. Vuran, and S. S. Aria, "Semi-supervised near-miss fall detection for ironworkers with a wearable inertial measurement unit," *Automation in Construction*, vol. 68, pp. 194–202, August 2016.

[3] K. Yang, C. R. Ahn, M. C. Vuran, and H. Kim, "Collective sensing of workers' gait patterns to identify fall hazards in construction," *Automation in Construction*, vol. 82, pp. 166–178, October 2017.

[4] K. Yang, C. Ahn, M. C. Vuran, and H. Kim, "Analyzing spatial patterns of workers gait cycles for locating latent fall hazards," in *Computing in Civil Engineering*, Seattle, WA, June 2017.

[5] K. Yedavalli, B. Krishnamachari, S. Ravula, and B. Srinivasan, "Ecolocation: a sequence based technique for RF localization in wireless sensor networks," in *Proc. Int. Symp. on Information processing in sensor networks (IPSN)*, Boise, ID, April 2005.

[6] N. Li, B. Becerik-Gerber, B. Krishnamachari, and L. Soibelman, "An environment-aware sequence-based localization algorithm for supporting building emergency response operations," in *Computing in Civil Engineering*, Los Angeles, CA, June 2013.

[7] K. Yedavalli and B. Krishnamachari, "Sequence-based localization in wireless sensor networks," *IEEE Trans. Mobile Comput.*, vol. 7, no. 1, pp. 81–94, January 2008.

[8] Y. Yu, C. Jiang, and Zhao., "Sequence-based localization algorithm with improved correlation metric and dynamic centroid," *Science China Information Sciences*, vol. 54, no. 11, pp. 2349–2358, November 2011.

[9] S. Deora and B. Krishnamachari, "Harnessing non-uniform transmit power levels for improved sequence based localization," in *Proc. IEEE DCOSS*, Marina Del Rey, CA, May 2014.

[10] D. Vasisht, S. Kumar, and D. Katabi, "Decimeter-level localization with a single WiFi access point," in *NSDI*, Santa Clara, CA, March 2016.

[11] M. Kotaru, K. Joshi, D. Bharadia, and S. Katti, "SpotFi: Decimeter level localization using WiFi," in *ACM SIGCOMM*, London, UK, August 2015.

[12] A. Bensky, *Wireless positioning technologies and applications*. Artech House, 2016.

[13] J. Yang, Y. Li, and W. Cheng, "An improved neighbor-correlation-extended-kalman-filter fusion method for indoor navigation," *Int. J. Distributed Sensor Networks*, vol. 13, no. 5, pp. 1–11, May 2017.

[14] M. Nilsson, J. Rantakokko, M. A. Skoglund, and G. Hendeby, "Indoor positioning using multi-frequency RSS with foot-mounted INS," in *Int. Conf. IPIN*, Busan, South Korea, October 2014.

[15] X. Zheng and H. Liu, "A study of localization accuracy using multiple frequencies and powers," *IEEE Trans. Parallel Distrib. Syst*, vol. 25, no. 8, pp. 1955–1965, August 2014.

[16] Y. Chapre, A. Ignjatovic, A. Seneviratne, and S. Jha, "CSI-MIMO: Indoor Wi-Fi fingerprinting system," in *Proc. IEEE Conf. on Local Computer Networks*, Edmonton, AB, September 2014.

[17] W. H. Press, *The art of scientific computing*. Cambridge university press, 1992.

[18] F. Guo, B. Zhou, and M. C. Vuran, "CFOSynt: Carrier frequency offset assisted clock syntonization for wireless sensor networks," in *Proc. IEEE INFOCOM 2017*, Atlanta, GA, May 2017.

[19] N. Scholastica, "Pathloss prediction model of a wireless sensor network in an indoor environment," *Int. J. Advanced Research in Electrical, Electronics and Instrumentation Engineering*, vol. 3, no. 9, pp. 11 665–11 673, September 2014.